Electronic Supplementary Material (ESI) for Journal of Materials Chemistry C.

Electronic Supplementary Information

High performance, electroforming-free, thin film memristors by using ionic $Na_{0.5}Bi_{0.5}TiO_3$

*Chao Yun[1], Matthew Webb[1], Weiwei Li[1], Rui Wu[1], Ming Xiao[1], Markus Hellenbrand[1], Ahmed Kursumovic[1], Hongyi Dou[2], Xingyao Gao[2], Samyak Dhole[3], Di Zhang[2], Aiping Chen[4], Jueli Shi[5], Kelvin H. L. Zhang[5], Haiyan Wang[2], Quanxi Jia[3], Judith. L. MacManus-Driscoll[1]**

S1. *I-V* curve for the 1st cycle and afterwards repetitions

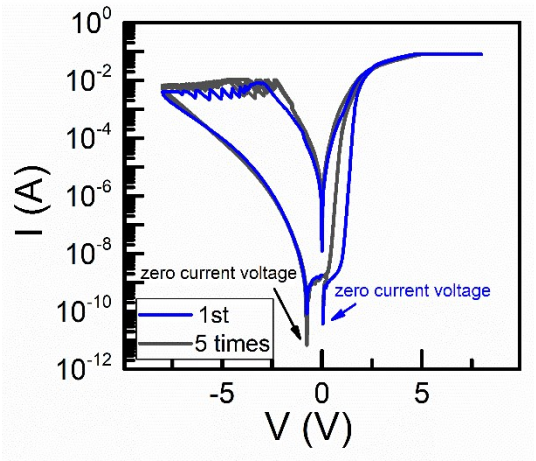

Fig. S1. *I-V* curves for the 1st cycle and 5 times repetition after the 1st cycle. The arrows indicate the zero current voltage position in each cycle.

It is noted that the very 1st cycle of the *I-V* curves shows slightly different behavior as compared with the consecutive *I-V* cycles, i.e. a slightly higher SET voltage. This occurs in other systems as well and is likely due to the formation of a built-in potentials after the 1st *I-V* cycle, which shifts the zero-current point to non-zero voltages.[1] This is not a forming process, as the forming process usually leads to partial dielectric breakdown and much higher conduction current and very different *I-V* shapes in the forming process which is not the case here.

S2. Distribution of R_{LRS} and R_{HRS}

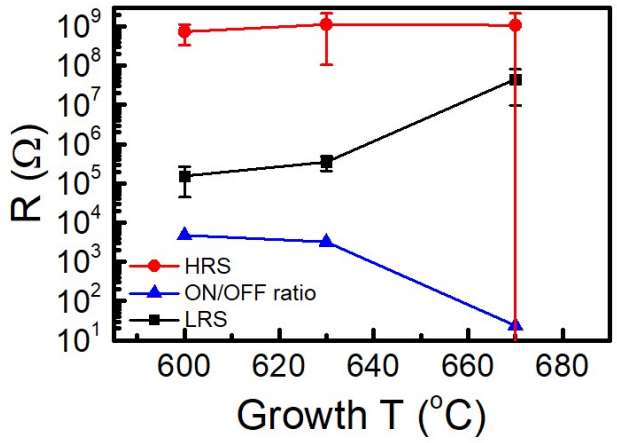

Fig. S2. Statistics for the R_{HRS}, R_{LRS} and ON/OFF ratios.

S3. Retention property of the Pt/NBT/Nb:STO resistive switching devices

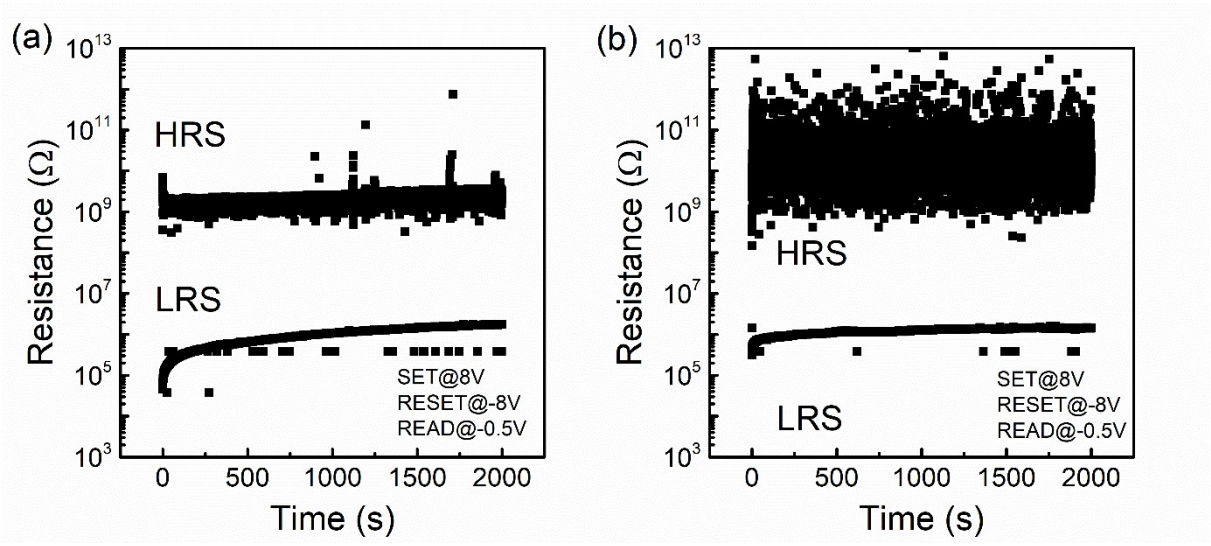

Fig. S3. Retention for the NBT samples grown at (a) 600 ℃ and (b) 630 ℃ over 20000 cycles.

S4. Switching speed and current response under voltage pulses

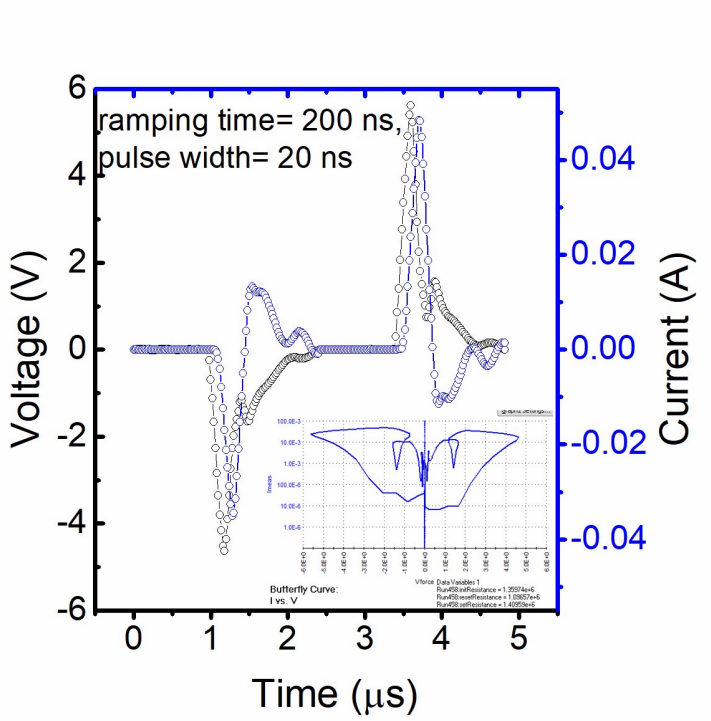

Fig. S4. Response of current under pulsed voltages under a voltage triangle pulse with 200 ns rise time and 20 ns pulse width. Inset is the butterfly *I-V* curve under the same pulsed voltage configuration.

S5. Current vs. Voltage characteristics of the Pt/NBT/Nb:STO samples in the pristine state

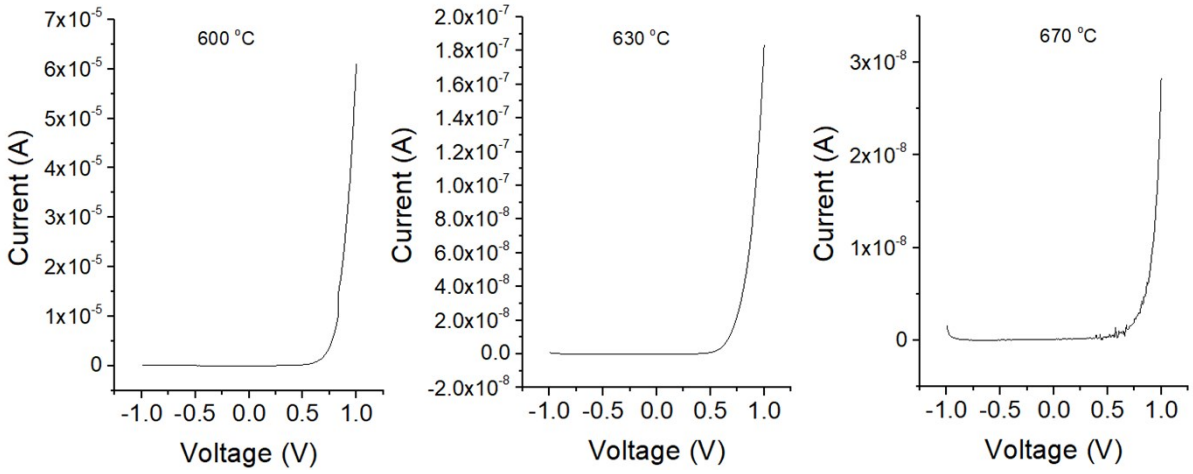

Fig. S5. *I-V* curves of the NBT samples from -1 to 1 V.

S6. Current vs. Voltage measurement of the Pt/Nb:STO/Ag sample

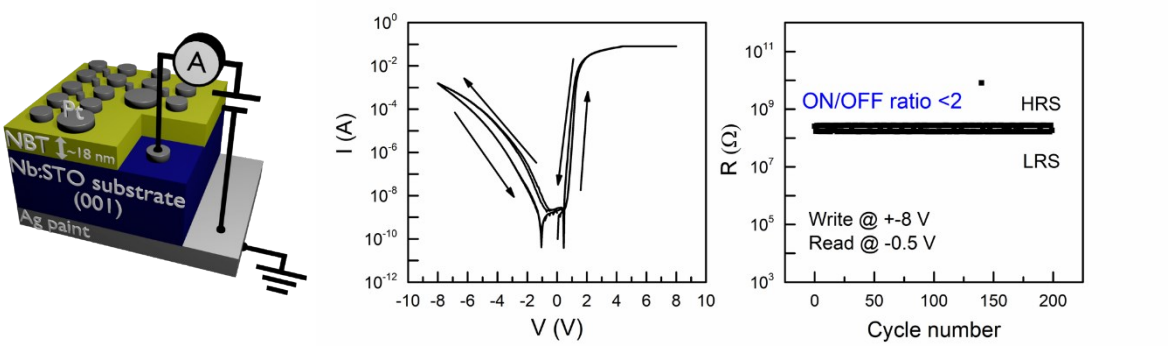

Fig. S6. Current-voltage characteristic of the Pt/Nb:STO/Ag sample. We placed the probe tips on the Pt electrode on the substrate surface of the same sample where there is no NBT film.

S7. Evidence of absence of Ag diffusion in the NBT/Nb:STO/Ag samples.

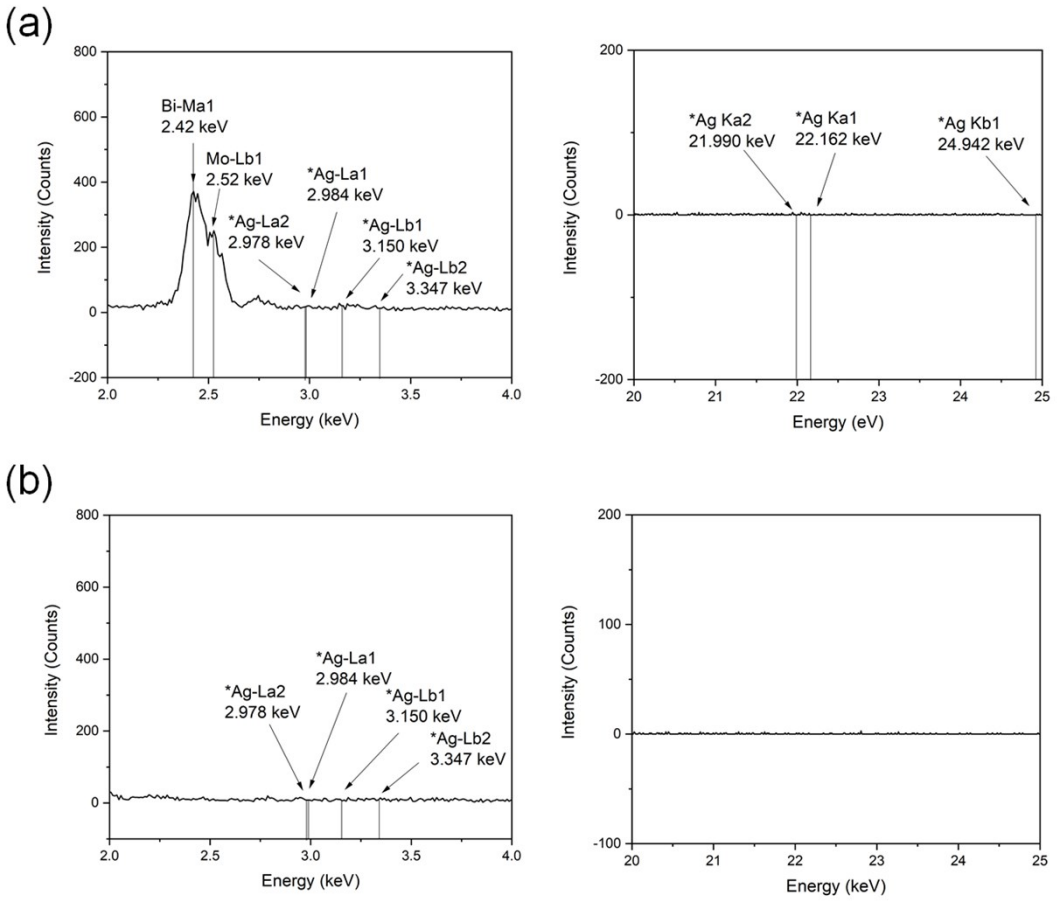

Fig. S7. EDX spectra for the NBT/Nb:STO samples taken from different areas: (a) one typical area from the NBT film and (b) one typical area from the substrate. The peak positions for Ag are all marked with *, which all indicates the absence of Ag element.

S8. Analysis on the relative stochiometric change of the NBT samples using XPS

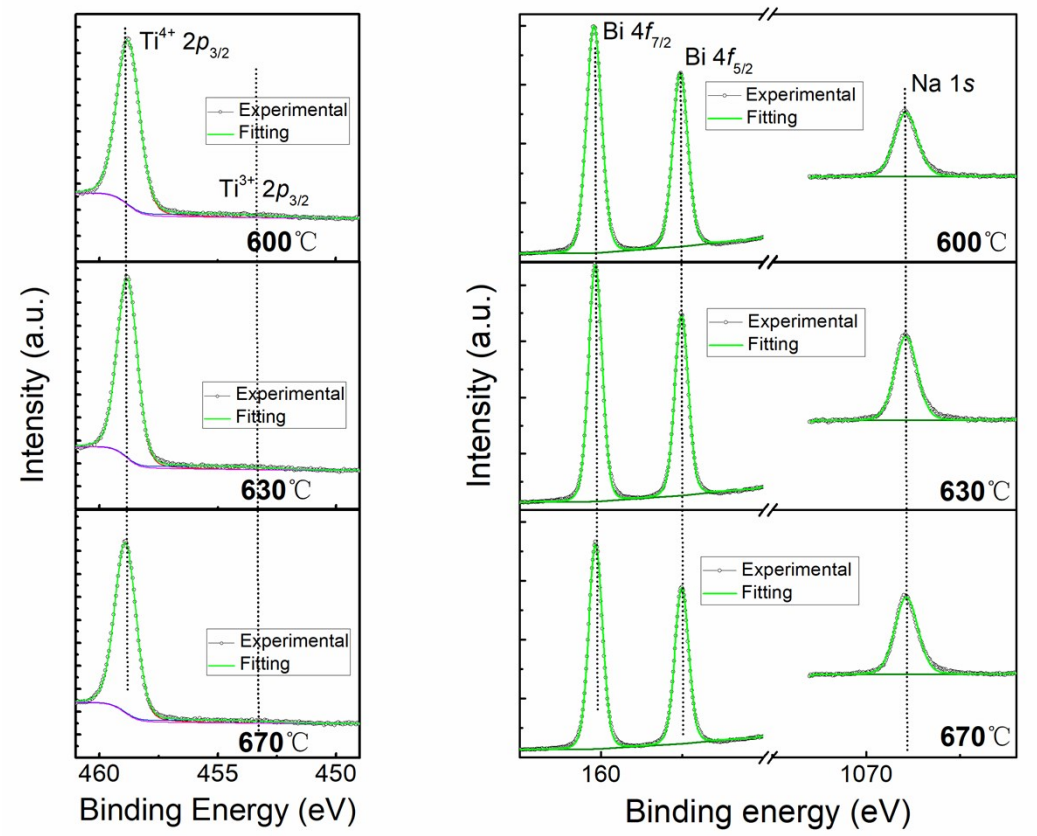

Fig. S8. XPS spectra for the (a) Ti 2*p* and (b) Bi 4*f* + Na 2*s*. The black dotted curves are experimental results and green lines are the fitted results.

S9. Analysis of conduction mechanism by *I-V* fitting

Having confirmed the direct correlation between cation non-stoichiometry and RS performance on a basis of no observed structural change (Fig. 1-Fig. 3), we turn to explain the mechanism of the resistive switching and the origin of the growth temperature dependent compositional tuning on the RS properties. To do this, we first perform fitting of the four branches of *I-V* curve in Fig. 1b to different conduction mechanisms. We focus on the low voltage region where the intrinsic conduction mechanism dominates.

Fig. S9a, b show the fitting in the low positive and negative voltage region (<1 V), which gives a linear relationship of log(*I*) vs. $V^{1/2}$. This indicates that the intrinsic current conduction is controlled by thermionic emission of electrons from the Schottky barrier to the conduction band of NBT. The current-voltage relationship is given by the following equation:

$$J = A^* T^2 exp\left[\frac{-e\left(\varphi_B - \sqrt{\frac{eE}{4\pi\varepsilon_r\varepsilon_0}}\right)}{kT}\right] \quad \text{(S1)}$$

$$A^* = \frac{4\pi q k^2 m^*}{h^3} = \frac{120 m^*}{m_0} \quad \text{(S2)}$$

where J is the current density, A^* is the effective Richardson constant, m_0 is the free electron mass, m^* is the effective electron mass in dielectric, T is the absolute temperature, e is the electronic charge, eφ_B is the Schottky barrier height (i.e. conduction band offset), E is the electric field, k is the Boltzmann constant, h is the Planck constant, ε_0 is the permittivity in a vacuum, and ε_r is the optical dielectric constant.

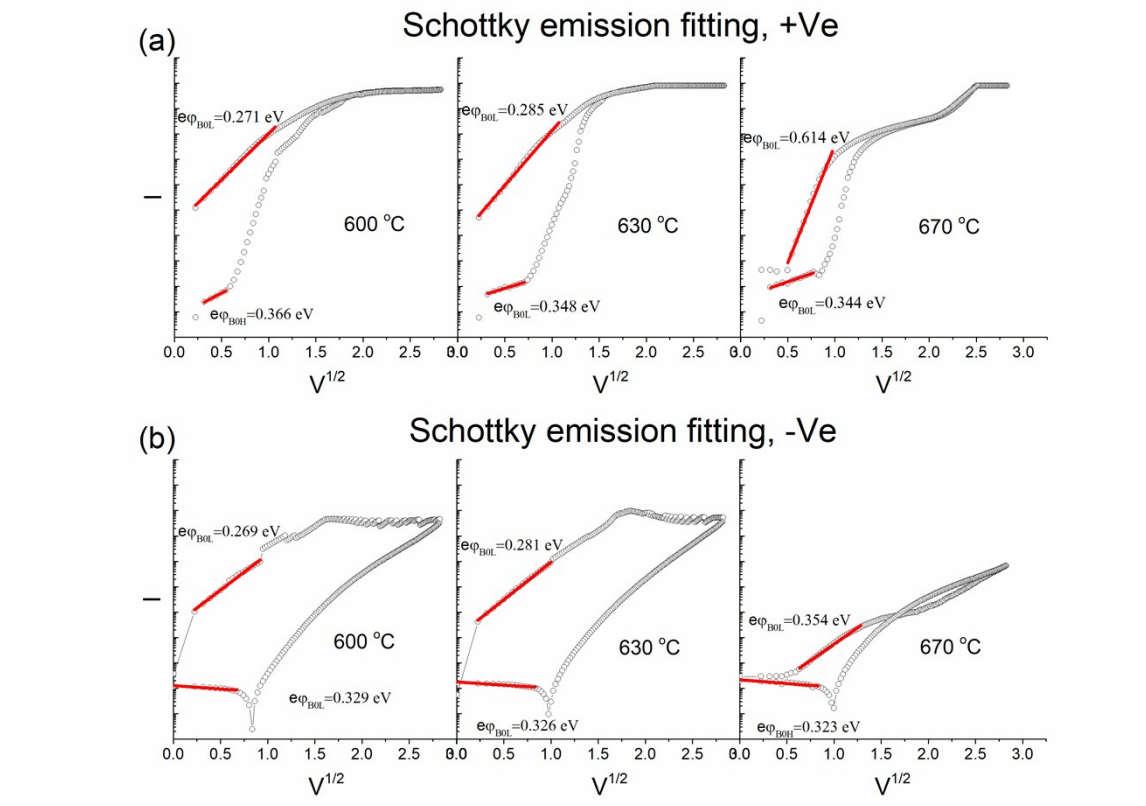

Fig. S9. Schottky emission fitting of the three samples for the (a) positive voltage branch and (b) negative voltage branch.

As discussed in the main text, probing the correlation between V_o and R_{LRS} (and R_{HRS}) is crucial to understand the reason for the optimised ON/OFF ratio for the 600 °C-grown film. Below, we analyse the influence of growth parameters on the R_{LRS} (R_{HRS}) values for the different growth temperatures. We list the relevant parameters of *I-V* fitting in Table S1, from which we see a correlation between the fitting parameters and the ON/OFF ratio with changing growth temperature, and then we discuss the possible origin for the modulated fitting parameters.

Table S1 Influence of growth temperature on RS parameters

Growth T (℃)	S_{Bi4f}/S_{Ti2p}	S_{Bi4f}/S_{Na1s}	$e\varphi_{B0H+}$ (eV)	$e\varphi_{B0H-}$ (eV)	R_{HRS}	$e\varphi_{B0L+}$ (eV)	$e\varphi_{B0L-}$ (eV)	R_{LRS}	Largest ON/OFF ratio
600	2.78	3.72	0.366	0.329	7.34e8± 4.04e8	0.271	0.269	1.54e6± 1.10e6	11250
630	2.49	2.81	0.348	0.326	1.12e9± 1.02e9	0.285	0.281	3.49e6± 1.40e6	5987
670	2.13	2.76	0.344	0.323	1.08e9± 1.08e9	0.614	0.354	4.54e7± 3.60e7	103

In the interface-limited Schottky emission process, the contact resistance determines the whole device resistance, which is directly reflected by non-bias (or built-in) barrier height $e\varphi_{B0}$.[2,3] $e\varphi_{B0}$ can be calculated by extrapolating the y-axis intercept of Schottky emission fitting curve. We calculated both the positive and negative branches of the *I-V* curves. As shown in Fig. S9a,b and as listed in Table S1, $e\varphi_{B0H}$ (denoted as $e\varphi_{B0H+}$ in branch 1 and $e\varphi_{B0H-}$ in branch 4) fitted at an initial state of low bias of HRS is almost constant ($e\varphi_{B0H+}$ decreases slightly from 0.366 to 0.344 eV and $e\varphi_{B0H}$- from 0.329 to 0.323 eV) with the increase of the growth temperature from 600 to 670 ℃. This is consistent with the nearly same R_{HRS}.

We also note that the $e\varphi_{B0L}$ fitted at low bias of LRS increases drastically ($e\varphi_{B0L+}$ from 0.271 to 0.614 eV and $e\varphi_{B0L}$- from 0.269 to 0.354 eV) with the increase in growth temperature, indicating a higher residual barrier height when the sweeping voltage switches off after SET process is finished. It is noted that the NBT sample grown at 670 °C shows a poor fitting and indicating other mechanism may contribute due to poor V_o migration. Considering that V_os are still accumulated near the interface after SET voltage is withdrawn and assuming no change of ε_r and m^* in the switching process, the increase in residual barrier height is consistent with the increase in R_{LRS} and decrease in ON/OFF ratio in the NBT samples with the increase in growth temperature.

As discussed above, the *mobile* V_o concentration is important for the effective lowering of the Schottky barrier when a positive bias is applied. One reason for the lower R_{LRS} and smaller $e\varphi_{B0L}$ in the lower temperature grown sample is a lower residual barrier height caused by a higher concentration of *mobile* V_o accumulating near the NBT/Nb:STO interface under positive bias.[4] Increased growth temperature causes an increase in cation (Bi) non-stoichiometry. When the amount of Bi vacancies

(V_{Bi}) increases further with the increase in growth temperature (Fig. 2), we see a drastic increase in R_{LRS} indicating a decrease in mobile V_o concentration. This can be explained considering that V_{Bi} forms defect association with V_o when V_{Bi} concentration is high. It is reported that V_o–V_{Bi} defect association has a high association energy at room temperature. [5,6] It is therefore likely that the concentration of *mobile* V_o decreases with the further increase in V_{Bi}. The decrease in *mobile* V_o with increasing film growth temperature results in less V_o accumulation near the NBT/Nb:STO interface and less effective decrease in the interfacial band bending upon application of positive bias. Hence the increase in R_{LRS} with growth temperature is well understood.

S10. Ionic conductivity of the NBT film

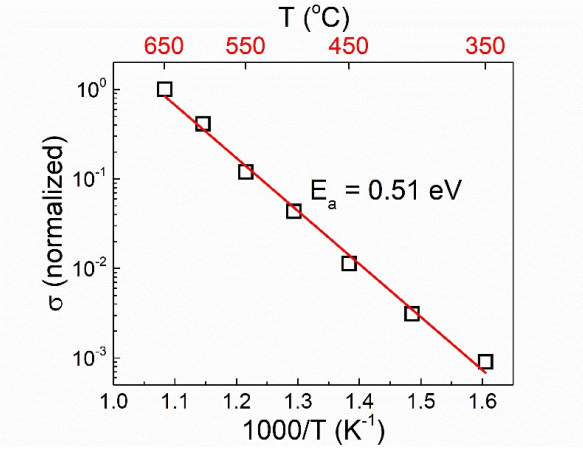

Fig. S10. Normalized ionic conductivity of the NBT film (grown at 600 °C) with temperature.

References

[1] X. Hong, D. J. Loy, P. A. Dananjaya, F. Tan, C. Ng, W. Lew, *J. Mater. Sci*. 2018, 53, 8720.

[2] A. Sawa, T. Fujii, M. Kawasaki, Y. Tokura, in Proc. SPIE 5932, *Strongly Correl. Electron Mater. Phys. Nanoeng*. (Eds: I. Bozovic, D. Pavuna), 2005, p. 59322C.

[3] A. Sawa, *Mater. Today* 2008, 11, 28.

[4] S. Cho, C. Yun, S. Tappertzhofen, A. Kursumovic, S. Lee, P. Lu, Q. Jia, M. Fan, J. Jian, H. Wang, S. Hofmann, J. L. MacManus-Driscoll, *Nat. Commun*. 2016, 7, 12373.

[5] L. Koch, S. Steiner, K.-C. Meyer, I.-T. Seo, K. Albe, T. Frömling, *J. Mater. Chem. C* 2017, 5, 8958.

[6] K.-C. Meyer, K. Albe, *J. Mater. Chem. A* 2017, 5, 4368.